

# Interchain-Frustration-Induced Metallic State in Quasi-One-Dimensional Mott Insulators

M. Tsuchiizu and Y. Suzumura

*Department of Physics, Nagoya University, Nagoya 464-8602, Japan*

C. Bourbonnais

*Département de Physique, Université de Sherbrooke, Sherbrooke, Québec, Canada J1K-2R1*

(Dated: January 29, 2007)

The mechanism that drives a metal-insulator transition in a undoped quasi-one-dimensional Mott insulator is examined in the framework of the Hubbard model with two different interchain hoppings  $t_{\perp 1}$  and  $t_{\perp 2}$  between nearest-neighbor chains defining an extremely anisotropic triangular lattice. By applying an  $N_{\perp}$ -chain renormalization group method at the two-loop level, we show how electron-electron umklapp scattering processes become irrelevant and a metallic state emerges when both  $t_{\perp 1}$  and  $t_{\perp 2}$  exceed some critical values. In the metallic phase, the quasi-particle weight becomes finite and is found to develop a strong momentum dependence. We discuss the temperature dependence of the resistivity due to umklapp scattering and the impact of our theory in the understanding of recent experiments on half-filled quasi-one-dimensional organic conductors.

PACS numbers: 71.10.Fd, 71.10.Pm, 71.30.+h

The remarkable properties of strongly correlated systems near a metal to Mott insulator (MI) transition stand out as one of the richest parts of the physics of strongly correlated systems [1]. This takes on particular importance in low dimensional materials at half-filling, and especially in one dimension, where spin and charge excitations are well known to be invariably decoupled, an effect that receives experimental confirmation in the one-dimensional (1D) oxide material  $\text{SrCuO}_2$  [2]. How this picture modifies when the hopping of electrons in more than one spatial direction progressively grows and a higher dimensional metallic ground state becomes possible is a key issue that remains poorly understood. This problem finds concrete applications in organic molecular compounds, which constitute very close realizations of 1D systems. This is the case notably of (TTM-TTP) $\text{I}_3$  and (DMTSA) $\text{BF}_4^-$  which, as genuine half-filled band materials due to the monovalent anions  $\text{I}_3^-$  and  $\text{BF}_4^-$ , see their Mott insulating state being gradually suppressed under pressure [3, 4]. Quite recently, resistivity measurements on (TTM-TTP) $\text{I}_3$  at high pressure revealed that the temperature scale for the Mott insulating behavior is suppressed by an order of magnitude down to  $T_{\text{MI}} \approx 20$  K at  $P = 8$  GPa of pressure, with a metallic ground state expected to occur above 10 GPa [5]. It is the objective of this letter to propose a theoretical description of this transition.

Bosonization, renormalization group (RG) approaches to the 1D Hubbard model in weak coupling and its exact solution from the Bethe ansatz [6, 7, 8], show that electron-electron umklapp scattering processes are a key ingredient that promotes the existence of a Mott insulating ground state at half-filling. The difficulty underlying the mechanism of the MI transition in the quasi-1D case resides in the fact that the decoupling of spin and charge excitations on the metallic side of the transition at higher dimension is absent, namely when Fermi liquid quasi-particles excitations appear. The MI transition for weakly coupled half-filled chains has been analyzed from the dynamical mean-field theory, extended to include

one-dimensional fluctuations (the chain-DMFT) [9] and from an RPA treatment of the interchain hopping [10]. Fermi surface nesting conditions, which couple to umklapp scattering, are altered in the quasi-1D case and become strongly momentum dependent, especially in the presence of frustration in the electron kinetics. These effects, which are non perturbative in the interchain hoppings, are not fully taken into account in these approaches and deserve further investigation.

In this Letter, we apply an  $N_{\perp}$ -chain RG approach to quasi-one-dimensional half-filled system as developed recently at the two-loop level [11, 12], and in which the momentum dependence of Fermi surface nesting and umklapp scattering can be included in a systematic way [13, 14, 15, 16]. To study the relative stability of the metallic vs Mott state, we examine the one-particle Green's function by including self-energy corrections that appear beyond the one-loop level of the RG.

We consider the quasi-one-dimensional half-filled Hubbard model on an anisotropic triangular lattice [Fig. 1(a)], with the transfer energies  $t_{\parallel} \gg |t_{\perp 1}|, |t_{\perp 2}|$  ( $t_{\parallel}$  is the energy along chains and  $t_{\perp 1}$  and  $t_{\perp 2}$  are those between chains). Our Hamiltonian, with the onsite Coulomb repulsion  $U$  is given by

$$\begin{aligned}
 H = & -t_{\parallel} \sum_{j,\ell,s} \left( c_{j,\ell,s}^{\dagger} c_{j+1,\ell,s} + \text{H.c.} \right) \\
 & - t_{\perp 1} \sum_{j,\ell,s} \left( c_{j,\ell,s}^{\dagger} c_{j,\ell+1,s} + \text{H.c.} \right) \\
 & - t_{\perp 2} \sum_{j,\ell,s} \left( c_{j,\ell,s}^{\dagger} c_{j+1,\ell+1,s} + \text{H.c.} \right) \\
 & + U \sum_{j,\ell} n_{j,\ell,\uparrow} n_{j,\ell,\downarrow} - \mu \sum_{j,\ell,s} c_{j,\ell,s}^{\dagger} c_{j,\ell,s}. \quad (1)
 \end{aligned}$$

The operator  $c_{j,\ell,s}$  denotes the annihilation of an electron on the  $j$ th site in the  $\ell$ th chain with spin  $s$ , and  $n_{j,\ell,s} = c_{j,\ell,s}^{\dagger} c_{j,\ell,s} - \frac{1}{2}$ . Here  $\ell = 1, \dots, N_{\perp}$  is the chain index. We take a continuum limit along the chain direction, whereas in the transverse direction we consider a finite system having an even number of chains  $N_{\perp}$  with the boundary condition

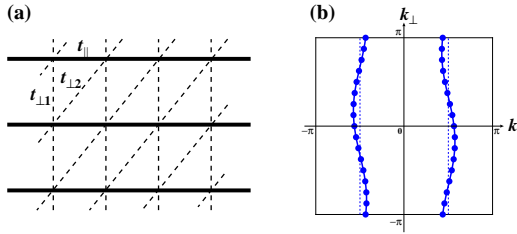


FIG. 1: (Color online) (a) Lattice geometry of the present model. (b) The corresponding Fermi surface where the case for  $N_{\perp} = 16$  is shown.

$c_{j,N_{\perp}+1,s} = c_{j,1,s}$ . By applying a Fourier transform, the kinetic term can be rewritten as  $H_0 = \sum_{\mathbf{k},s} \varepsilon(\mathbf{k}) c_s^{\dagger}(\mathbf{k}) c_s(\mathbf{k})$ , where  $\mathbf{k} \equiv (k_{\parallel}, k_{\perp})$  and the energy dispersion is given by  $\varepsilon(\mathbf{k}) = -2t_{\parallel} \cos k_{\parallel} - 2t_{\perp 1} \cos k_{\perp} - 2t_{\perp 2} \cos(k_{\parallel} + k_{\perp}) - \mu$ . For  $|t_{\perp i}| \ll t_{\parallel}$ , the right- and left-moving electrons in the 1D case are well-defined due to an open Fermi surface (Fig. 1) and the shape of the Fermi surface can be parametrized by the transverse momentum  $k_{\perp}$  [11]. To lowest order in the inter-chain hoppings  $t_{\perp 1}$  and  $t_{\perp 2}$ , the Fermi surfaces for right (+) and left (-) moving electrons, as a function of  $k_{\perp}$ , are given by

$$k_F^{\pm}(k_{\perp}) = \pm \frac{\pi}{2} \pm \frac{t_{\perp 1}}{t_{\parallel}} \cos k_{\perp} - \frac{t_{\perp 2}}{t_{\parallel}} \sin k_{\perp}, \quad (2)$$

and the chemical potential is  $\mu = O(t_{\perp i}^2)$ . The form of Eq. (2) is not specific to the present model (1), but is general if one neglects higher-order corrections such as  $\cos 2k_{\perp}$ . By consid-

ering the weak-interacting case and neglecting the  $k_{\perp}$  dependence of the velocity, the linearized dispersion used in the RG method takes the simple form:  $\varepsilon_p(\mathbf{k}) = pv[k_{\parallel} - k_F^p(k_{\perp})]$  with  $v = 2t_{\parallel}$  and  $p = \pm$ .

We follow closely the formulation of the two-loop RG method of Ref. 11 and first introduce the  $g$ -ology coupling constants [see Eq. (2.8) in Ref. 11], namely the backward ( $g_{1\perp}$ ), forward ( $g_{2\perp}$ ), and umklapp ( $g_{3\perp}$ ) scatterings with opposite spins, and the forward scattering ( $g_{\parallel}$ ) and umklapp ( $g_{3\parallel}$ ) scatterings for parallel spins. The coupling constants are renormalized differently, developing an external – transverse – momenta dependence in the vertex corresponding to a patch-index dependence; that is,  $g_{\nu} \rightarrow g_{\nu(q_{\perp}, k_{\perp 1}, k_{\perp 2})}$ , where  $k_{\perp 1}$  and  $k_{\perp 2}$  are the transverse momenta for the right-going fermions, and  $q_{\perp}$  is the momentum transfer [11]. In terms of the Hubbard interaction  $U$ , the magnitude of the initial couplings are given by  $g_{1\perp(q_{\perp}, k_{\perp 1}, k_{\perp 2})} = g_{2\perp(q_{\perp}, k_{\perp 1}, k_{\perp 2})} = g_{3\perp(q_{\perp}, k_{\perp 1}, k_{\perp 2})} = U$  and  $g_{\parallel(q_{\perp}, k_{\perp 1}, k_{\perp 2})} = g_{3\parallel(q_{\perp}, k_{\perp 1}, k_{\perp 2})} = 0$ . To simplify the notation, we omit in the following the  $\perp$  index for transverse momenta. As in the 1D case, the physical picture becomes more transparent by introducing the new set of couplings:  $g_{\rho(q, k_1, k_2)} \equiv [g_{2\perp(q, k_1, k_2)} + g_{\parallel(q, k_1, k_2)}]$ ,  $g_{\sigma(q, k_1, k_2)} \equiv [g_{2\perp(q, k_1, k_2)} - g_{\parallel(q, k_1, k_2)}] = g_{1\perp(q, k_1, k_2)}$ ,  $g_{c(q, k_1, k_2)} \equiv g_{3\perp(q, k_1, \pi - k_2)}$ , and  $g_{cs(q, k_1, k_2)} \equiv g_{3\parallel(q, k_1, \pi - k_2)}$ , for the charge ( $\rho, c$ ) and spin ( $\sigma, s$ ) sectors.

The RG equations are derived by scaling the bandwidth cut-off  $\Lambda (= 2vk_F)$  as  $\Lambda_l = \Lambda e^{-l}$ , where  $l$  is the scaling parameter. Up to the one-loop level, the RG equation for the coupling of the umklapp scattering is given by

$$\begin{aligned} \frac{d}{dl} G_{c(q, k_1, k_2)} = & + \frac{1}{2N_{\perp}} \sum_{k'} \{ [G_{\rho(q, k_1, k')} - 3G_{\sigma(q, k_1, k')}] G_{c(q, k', k_2)} + 2G_{\sigma(q, k_1, k')} G_{c(\pi - q + k' + k_2, k', k_2)} \} I''_{(q, k', k_1, k_2)} \\ & + \frac{1}{2N_{\perp}} \sum_{k'} [G_{\rho(\pi - q + k_1 + k_2, k_1, k')} + G_{\sigma(\pi - q + k_1 + k_2, k_1, k')}] G_{c(q - k_1 + k', k', k_2)} I''_{(\pi - q + k_1 + k_2, k', k_1, k_2)}, \end{aligned} \quad (3)$$

where  $I''_{(q, k', k_1, k_2)} = \frac{1}{2} F(A_{q, k', k_1}/\Lambda) + \frac{1}{2} F(A'_{q, k', k_2}/\Lambda)$  with  $F(x)$  being a cutoff function satisfying  $F(x) = 1$  for  $|x| \lesssim 1$  and  $F(x) = 0$  for  $|x| \gg 1$ . The quantities  $A_{q, k', k_i}$  and  $A'_{q, k', k_i}$  are given by  $A_{q, k', k_i}^{(\prime)} \equiv 2t_{\perp 1}[\cos k' + \cos(k' - q)] - 2t_{\perp 1}[\cos k_i + \cos(k_i - q)] - 2t_{\perp 2}[\sin k' - \sin(k' - q)] + (-)2t_{\perp 2}[\sin k_i - \sin(k_i - q)]$ . The explicit forms of the two-loop RG equations for all coupling constants in the case  $t_{\perp 2} = 0$  are given in Ref. [11]. We solve here these two-loop RG equations numerically for a system with  $N_{\perp} = 16$ . For even  $N_{\perp}$ , the solution of the RG flows indicates the existence of a finite spin gap in the low-energy limit, a gap that is expected to vanish in the infinite  $N_{\perp}$  limit. The characteristic scale  $l_{N_{\perp}}$  above which finite size effect would appear can be roughly estimated to be  $l_{N_{\perp}} \approx \ln[\Lambda/|t_{\perp i} \sin(2\pi/N_{\perp})|]$ . For

the noninteracting case with  $N_{\perp} = 16$  and  $t_{\perp 1}/t_{\parallel} = 0.1$ , this scale reaches  $l_{N_{\perp}} \approx 5$ , while the crossover scale [11] is  $l_{\perp} \approx \ln(\Lambda/t_{\perp 1}) \approx 4$ .

For the bipartite lattice ( $t_{\perp 2} = 0$ ), the system remains always insulating even for large  $t_{\perp 1}$  [11]. This is due to perfect nesting condition for the Fermi surface. In this case the inter-chain hopping  $t_{\perp 1}$  is relevant and becomes large under scaling procedure, and some of the umklapp couplings becomes small. However, a macroscopic number of umklapp couplings remains relevant due to perfect nesting at vector  $\mathbf{Q} = (\pi, \pi)$ . In the case of large  $t_{\perp 2}$ , these remaining relevant umklapp scatterings are strongly reduced and all the umklapp scatterings remain weak. This implies that the charge gap collapses and a metallic state emerges as a consequence of nesting de-

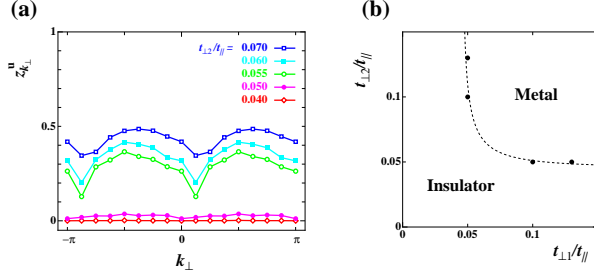


FIG. 2: (Color online) (a) Umklapp-scattering contribution of the quasi-particle weight  $z_{k_\perp}^u$  for  $U/t_\parallel = 2$ ,  $N_\perp = 16$ ,  $t_{\perp 1}/t_\parallel = 0.1$  with several  $t_{\perp 2}$ . (b) Ground-state phase diagram on the plane of  $t_{\perp 1}/t_\parallel$  and  $t_{\perp 2}/t_\parallel$ . The dotted line denotes the condition of Eq. (5).

viations of the Fermi surface due to the large interchain frustration.

One-particle properties are best studied through the quasi-particle weight  $z_{k_\perp}$ . Based on the two-loop RG method [11], the quasi-particle renormalization factor weight factorizes as  $z_{k_\perp} \equiv z_{k_\perp}^n z_{k_\perp}^u$ , where  $z_{k_\perp}^n$  and  $z_{k_\perp}^u$  are the contributions from the normal and umklapp scattering, respectively. Their explicit forms read [11]

$$z_k^{n(u)} = \exp \left[ -\frac{1}{2N_\perp^2} \sum_{q,k'} \int_0^\infty dl G_{\Sigma n(u)(q,k,k')}^2 J_{1(q,k,k')}^{n(u)} \right], \quad (4)$$

where  $G_{\Sigma n}^2$  and  $G_{\Sigma u}^2$  denote the coupling constants  $G_{\Sigma n(q,k,k')}^2 \equiv \frac{1}{2}[G_{\rho(q,k,k')}^2 + 3G_{\sigma(q,k,k')}^2]$  and  $G_{\Sigma u(q,k,k')}^2 \equiv G_{c(q,k,k')}^2 + G_{c(\pi-q+k+k',k,k')}^2 - G_{c(q,k,k')}G_{c(\pi-q+k+k',k,k')}$  with  $G_\nu = g_\nu/(2\pi v)$ . The quantities  $J_{1(q,k,k')}^n$  and  $J_{1(q,k,k')}^u$  are cutoff functions that depend on  $A_{q,k,k'}$  and  $A'_{q,k,k'}$ , respectively. In order to analyze one-particle features of the MI transition, one can focus on the umklapp contribution  $z_{k_\perp}^u$ , since  $z_{k_\perp}^n$  always remains finite for  $l < l_{N_\perp}$  in the metallic state. The  $k_\perp$  dependence of the umklapp scattering contribution to  $z_{k_\perp}$  for several values of  $t_{\perp 2}$  at fixed  $t_{\perp 1}/t_\parallel = 0.1$  is shown in Fig. 2. For weak frustration  $t_{\perp 2}(< t_{\perp 2}^c)$ , this quantity is small showing the existence of an insulating phase with no low-energy quasi-particles. On the other hand, for strong frustration  $t_{\perp 2}(> t_{\perp 2}^c)$ , it takes sizable values and shows a strong  $k_\perp$  dependence. In the proximity of the insulating phase, the quantity  $z_{k_\perp}^u$  presents a broad maximum around  $k_\perp \approx \pm\pi/2$ , which behavior implies the emergence of Fermi pockets [10], or ‘cold’ regions around  $\mathbf{k} \approx (k_F^p(\pm\pi/2), \pm\pi/2)$  [13, 14]. The dips or ‘hot spots’ in the quasi-particle weight correspond to regions of the Fermi surface where the nesting conditions remain the most favorable. The overall profile, which differs from previous analysis [9, 10], is then intrinsically linked to the momentum dependent nesting properties over the whole Fermi surface [16].

The boundary for the metal-insulator transition can be determined analytically by noting that the metallic phase of the RG analysis is linked to the irrelevance of umklapp scattering. The metallic phase boundary can thus be obtained when

the energy scale of imperfect nesting for umklapp scatterings becomes comparable to the energy scale  $\Delta_\rho^{1D}$  of the 1D Mott gap. By noting that the nesting vector of the particle-hole loop, which couples to umklapp, is given by  $\mathbf{Q} = (\pi, \pi \pm 2\alpha)$  with  $\tan \alpha = t_{\perp 2}/t_{\perp 1}$ , the degree of the imperfect nesting (the amplitude of the quantity  $A'_{\pi \pm 2\alpha, k, k'}$ ) becomes  $\sqrt{t_{\perp 1}^2 + t_{\perp 2}^2} \sin 2\alpha$ . The phase boundary for the MI transition is then determined by the condition

$$\frac{t_{\perp 1}t_{\perp 2}}{\sqrt{t_{\perp 1}^2 + t_{\perp 2}^2}} = c\Delta_\rho^{1D} \quad (5)$$

where  $c$  is a numerical constant being of the order of unity. The small difference between the numerical results and the above analytical expression comes from the renormalization of the interchain hopping due to the normal scattering processes. The Mott gap is also renormalized by interchain hopping. The ground-state phase diagram on the plane of  $t_{\perp 1}/t_\parallel$  and  $t_{\perp 2}/t_\parallel$  is shown in Fig. 2(b), where the dotted line denotes Eq. (5). The ambiguities in the cutoff functions of the RG [11, 15], prevent us from obtaining a precise location of the phase boundary.

The Mott transition has also been addressed in two-dimensional Hubbard model on an anisotropic triangular lattice with nearest-neighbor hopping  $t$  and next-nearest neighbor hopping  $t'$  [17, 18]. A transition from an insulator without magnetic ordering to a paramagnetic metal was obtained by changing the hopping parameters. The present model (1) can be connected to the two-dimensional Hubbard model by taking  $t_\parallel \rightarrow t$ ,  $t_{\perp 1} \rightarrow t$ , and  $t_{\perp 2} \rightarrow t'$ . While our approach is restricted to the case where interchain hopping is small, the metal-insulator transition obtained here for finite frustration is consistent with the numerical results.

From the solution of the scaling flows of the umklapp scatterings, the temperature dependence of the resistivity can be qualitatively calculated from the memory function approach combined with the RG method by using  $l = \ln(\Lambda/T)$  [8, 19]. By extending the approach to the quasi-1D case, the perturbative expression of the conductivity reads  $\rho(T) \propto N_\perp^{-3} \sum_{q,k,k'} G_{c(q,k,k')}^2(l) e^{-l}$ . While this formula is not valid for large  $t_{\perp 1}/T$  [19], it will depict the qualitative temperature dependence of resistivity. Typical behaviors of the resistivity obtained from this formula are shown in Fig. 3(a), where the metallic behavior is verified for strong frustration. A phase diagram can be obtained from this behavior, as shown schematically in Fig. 3(b). At high temperature, the Tomonaga-Luttinger (TL) state is realized, which is followed in the crossover region by the development of a Fermi surface. The effect of the frustration is yet masked by thermal fluctuations, which means that this region can be described by an effective nested Fermi surface. It can also be seen from Fig. 3(a) that the characteristic temperature at which the crossover to the metallic Fermi liquid state takes place increases with  $t_{\perp 2}$ .

We would like to discuss here the impact of our results on the understanding of the phase diagram of the quasi-1D

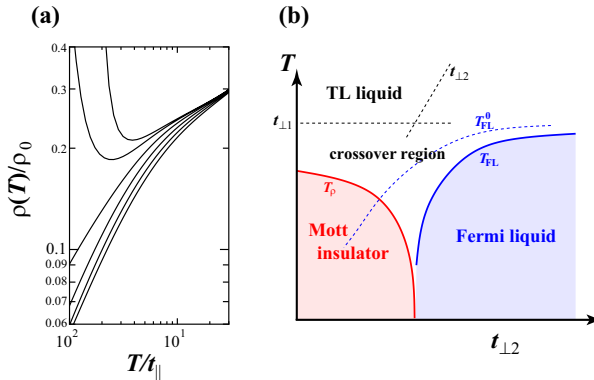


FIG. 3: (Color online) (a) Temperature dependence of the resistivity for  $N_{\perp} = 16$ ,  $t_{\perp 1}/t_{\parallel} = 0.1$ , and  $U/t_{\parallel} = 1.5$  with fixed  $t_{\perp 2}/t_{\parallel} = 0, 0.02, 0.04, 0.06, 0.08, 0.10$  (from top to bottom), and  $\rho_0 = \rho(\Lambda)$ . (b) Schematic illustration of the  $t_{\perp 2}$ - $T$  phase diagram, where  $T_p$  ( $T_{FL}$ ) represents the crossover temperature to the Mott insulator (metallic Fermi liquid).  $T_{FL}^0$  represents the bare temperature scale for imperfect nesting [left of Eq. (5)], which is reduced to  $T_{FL}$  due to the umklapp scattering processes.

molecular compound (TTM-TTP)I<sub>3</sub> under pressure [5]. The extended Hückel calculations [20] indicate that for (TTM-TTP)I<sub>3</sub>, there are two kinds of interchain transfer integrals, namely  $t_{\perp 1} \approx 9$  meV, and  $t_{\perp 2} \approx 6$  meV, which are nearly of the same order of magnitude and also small compared to  $t_{\parallel} \approx 260$  meV [21]. This emphasizes the pronounced hopping frustration of this quasi-1D compound. The Coulomb repulsion between electrons on the same molecular orbital of TTM-TTP is weak, and the estimated magnitude,  $U \approx 0.57$  eV [3], leads to the weak coupling magnitude  $U/t_{\parallel} \approx 2.2$ . From these figures, the energy scale for imperfect nesting [left-hand side of Eq. (5)] turns out to be about 5 meV. As for the magnitude of the charge gap at ambient pressure, we obtain  $\Delta_{\rho}^{1D} \approx 60$  meV, in fair agreement with the measured activation energy of resistivity at ambient pressure [3]. The bandwidth goes up under pressure, which decreases the ratio  $U/t_{\parallel}$  and in turn the charge gap. To reduce the gap at  $\Delta_{\rho}^{1D} \approx 5$  meV, namely down to the scale of imperfect nesting, one has roughly to double the hopping amplitudes. This represents a reasonable increase of band parameters under 8 GPa of pressure [22], and is consistent with the existence of a MI transition in (TTM-TTP)I<sub>3</sub> [5]. Finally, we note that at ambient pressure, below  $T_c \simeq 120$  K, this compound develops a non magnetic state (likely of the spin-Peierls type), which comes with an *intra-molecular* charge disproportionation (CD) [4]. However, since the resistivity already shows an insulating behavior above  $T_c$ , the present system can be indeed considered as a Mott insulator rather than a charge-ordered insulator, and the CD can be accounted for by dimerization of the tilted TTM-TTP molecules.

In summary, we have examined the effect of interchain frustration on the half-filled quasi-1D Hubbard chains by apply-

ing an  $N_{\perp}$ -chain two-loop RG method. The triangular lattice geometry of the system is found to be a key factor in the stability of the Mott insulating state and whenever the alteration of nesting conditions due to frustration in the transverse hoppings reaches some threshold a metallic state is restored. Our results find direct application to the description of temperature-pressure phase diagram of frustrated low dimensional half-filled organic compounds.

One of the authors (M.T.) thanks S. Yasuzuka, T. Kawamoto, T. Mori, A. Läuchli, and T. Giamarchi for valuable discussions. This work was supported in part by a Grant-in-Aid for Scientific Research on Priority Areas of Molecular Conductors (No. 15073213) from the Ministry of Education, Science, Sports, and Culture, Japan.

---

- [1] M. Imada, A. Fujimori, and Y. Tokura, Rev. Mod. Phys. **70**, 1039 (1998).
- [2] B.J. Kim *et al.*, Nature Phys. **2**, 397 (2006).
- [3] T. Mori *et al.*, Phys. Rev. Lett. **79**, 1702 (1997).
- [4] T. Mori, Chem. Rev. **104**, 4947 (2004).
- [5] S. Yasuzuka *et al.*, J. Phys. Soc. Jpn. **75**, 053701 (2006); J. Low. Temp. Phys. **142**, 197 (2006).
- [6] I. E. Dzyaloshinskii and A. I. Larkin, Sov. Phys. JETP, **34**, 422 (1972).
- [7] C. Bourbonnais, B. Guay and R. Wortis, in *Theoretical Methods for Strongly Correlated Electrons* eds. D. Sénéchal, A. M. Tremblay and C. Bourbonnais (New York, Springer, 2003) p. 77.
- [8] T. Giamarchi, *Quantum Physics in One Dimension* (Oxford University Press, New York, 2004).
- [9] S. Biermann *et al.*, Phys. Rev. Lett. **87**, 276405 (2001); T. Giamarchi *et al.*, J. Phys. IV France **114**, 23 (2004); C. Berthod *et al.*, Phys. Rev. Lett. **97**, 136401 (2006).
- [10] F. H. L. Essler and A. M. Tsvelik, Phys. Rev. B **65**, 115117 (2002).
- [11] M. Tsuchiizu, Phys. Rev. B **74**, 155109 (2006).
- [12] M. Tsuchiizu, Y. Suzumura, and C. Bourbonnais, to be published in J. Phys. Cond. Mat.
- [13] R. Duprat and C. Bourbonnais, Eur. Phys. J. B **21**, 219 (2001).
- [14] C. Bourbonnais and R. Duprat, J. Phys. IV France **114**, 3 (2004).
- [15] S. Dusuel and B. Douçot, Phys. Rev. B **67**, 205111 (2003).
- [16] D. Rohe and A. Georges, cond-mat/0608032.
- [17] T. Kashima and M. Imada, J. Phys. Soc. Jpn. **70**, 3052 (2001); H. Morita, S. Watanabe and M. Imada, *ibid.* **71**, 2109 (2002).
- [18] B. Kyung and A. -M. S. Tremblay, Phys. Rev. Lett. **97**, 046402 (2006).
- [19] T. Giamarchi, Phys. Rev. B **44**, 2905 (1991).
- [20] T. Mori *et al.*, Bull. Chem. Soc. Jpn. **67**, 661 (1994);
- [21] T. Kawamoto, Typographical error in the Table 4 of Ref. 20 is pointed out. The correct overlap integral of the [10̄2] direction is 0.09.
- [22] This corresponds to an increase of 20%/GPa, or so for the transfer integrals under hydrostatic pressure, which is a typical figure in quasi-1D organic conductors. See for example, D. Jérôme and H. J. Schulz, Adv. Phys. **31**, 299 (1982).